

Effect of small amount of ultra high molecular weight component on the crystallization behaviors of bimodal high density polyethylene

Shijie Song^a, Peiyi Wu^a, Minxing Ye^{a,b}, Jiachun Feng^{a,*}, Yuliang Yang^a

^a Key Laboratory of Molecular Engineering of Polymers, Ministry of Education, Department of Macromolecular Science, Fudan University, 220 Handan Road, Shanghai 200433, China

^b Department of Materials Science, Fudan University, Shanghai 200433, China

ARTICLE INFO

Article history:

Received 4 January 2008

Received in revised form 2 April 2008

Accepted 26 April 2008

Available online 2 May 2008

Keywords:

Polyethylene

Crystallization

Nucleation

ABSTRACT

In order to clarify the effect of high molecular weight component on the crystallization of bimodal high density polyethylene (HDPE), a commercial PE-100 pipe resin was blended with small loading of ultra high molecular weight polyethylene (UHMWPE). The isothermal crystallization kinetics and crystal morphology of HDPE/UHMWPE composites were studied by differential scanning calorimetry (DSC) and polarized optical microscopy (POM), respectively. The presence of UHMWPE results in elevated initial crystallization temperature of HDPE and an accelerating effect on isothermal crystallization. Analysis of growth rate using Lauritzen–Hoffman model shows that the fold surface free energy (σ_e) of polymer chains in HDPE/UHMWPE composites was lower than that in neat HDPE. Morphological development during isothermal crystallization shows that UHMWPE can obviously promote the nucleation rate of HDPE. It should be reasonable to conclude that UHMWPE appeared as an effective nucleating agent in HDPE matrix. Rheological measurements were also performed and it is shown that HDPE/UHMWPE composites are easy to process and own higher melt viscosity at low shear rate. Combining with their faster solidification, gravity-induced sag in practical pipe production is expected to be effectively avoided.

© 2008 Elsevier Ltd. All rights reserved.

1. Introduction

Since its first introduction in pipe application over 40 years ago, polyethylene (PE) has been taking a growing place in transportation and distribution of water and gas. PE pipes offer distinct advantages compared with other piping materials because they are lightweight, corrosion-free, exhibit very high ductility and allow all-welded construction [1]. First- and second-generation PE pipe resins for water and gas distribution are known as PE-63 and PE-80, which must withstand a minimum required hoop stresses of 6.3 MPa and 8.0 MPa for up to 50 years at 20 °C, respectively. Driven by the advancement in catalyst and polymerization technology, the third-generation PE pipe resins called “bimodal” resins have emerged since 1990s, and are classified to PE-100 (i.e., pipe must withstand hoop stress of 10 MPa for up to 50 years at 20 °C, see ISO 12162). The molecular feature that allows these bimodal resins to exhibit improved properties is not the shape of the molecular weight distribution (MWD) but the preferred incorporation of comonomers in the long polymer chains within the second reactor during a cascade polymerization process. This way a polymer blend is formed with low-molecular weight ethylene homopolymer components and

high-molecular weight ethylene-1-alkene copolymer components [2–4]. Bohm [3] has recently concluded that in a bimodal PE-100 resin, the high-molecular weight copolymers form amorphous regions and act as tie molecules that connect the crystal lamella mainly formed by the low-molecular weight homopolyethylene. In this manner, a physical network is formed and thus the mechanical properties of the polymer are greatly improved.

However, compared with unimodal resins, bimodal PE-100 resins lack the melt elasticity due to the absence of both long chain branching (LCB) and the very high molecular weight tail [4]. The result is that PE-100 resins are limited in producing large diameter, thick wall pipes because the molten polymers tend to sag before hardening. Another problem with pipe fabrication is the thermal gradient across the pipe wall during extrusion process. The outside and inside surfaces are cooled down by a water spray and solidified quickly. But the crystallization (shrinkage) of the core region is much slower which causes residual stress within a pipe [5]. Industrially, it has been widely accepted that accelerating the crystallization rate of PE pipe resins could effectively avoid sag due to the fast hardening of the molten polymers. Meanwhile, if the overall crystallization rate is increased, the residual stress within a pipe will decrease because the differences in shrinkage between surface and core region of the pipe wall become inconspicuous.

The crystallization of polymer is an important physical process and remains a hot issue. Many methods, models as well as

* Corresponding author. Tel.: +86 21 6564 3735; fax: +86 21 6564 0293.
E-mail address: jcfeng@fudan.edu.cn (J. Feng).

technologies have been invented aiming to describe the whole process of crystallization from the very beginning to the late stage and clarify the mechanism behind it. Recently, the early stages of crystallization in polyethylene have been explored by some researchers [6–8] using various techniques and Bassett [9] studied a new linear nucleation and oriented crystallization of PE. It is widely accepted that the crystallization of polymers such as PE and polypropylene (PP) is mainly controlled by the nucleation stage. Using some specific nucleating agents to shorten the inducing time of crystallization and accelerate the formation of crystalline nuclei is a technique that is commonly applied in polymer industry. However, unlike PP, there are few commercial nucleating agents for PE. Therefore, how to promote the crystallization of bimodal PE pipe resins has been a challenging problem both for academe and industry.

UHMWPE is one of the leading plastics that have been developed in recent decades. The outstanding properties of UHMWPE, such as toughness, high wear strength, and abrasion resistance, provide not only new utilities but also scientific interests. UHMWPE has been widely used to optimize the property of polymers such as PE, PP, ethylene-propylene-ternary (EPT) rubber, polyaniline (PANI) and polyacrylate (PA) [10–15]. Recently, Busby et al. [16] obtained a novel nanostructured polymeric composite of polycarbonate (PC) and UHMWPE via a supercritical-fluid route. With regard to the blending of HDPE and UHMWPE, many research works have already been reported elsewhere [17–21,24,25]. For example, Tincer and Coskun [17] have prepared the blends of HDPE/UHMWPE at different compositions and mixing rates to study their mechanical properties, thermal oxidative degradation and morphologies. Lim et al. [20,21] have studied the suitability of HDPE/UHMWPE composites as biomaterials. However, most of these works were focused on mechanical or processing properties. As UHMWPE owns a high melt viscosity and can be drawn even from a melt, special morphology such as shish-kebab can be formed during the crystallization of UHMWPE [22,23]. Accordingly, whether UHMWPE will have a special influence on crystallization behaviors of bimodal HDPE is an interesting problem and has not been well understood up to date, although some investigations have paid attention to the crystallization behavior of HDPE/UHMWPE composite under shear [26–28].

In our previous studies [29,30], using self-consistent mean field theory, it has been found that, for the case of a binary polymer blend, broadening MWD would decrease the energy barrier of nucleation and theoretically the high molecular weight component has the capability of inducing nucleation. Therefore, if UHMWPE could act as a certain nucleating agent for bimodal HDPE pipe resins and accelerate their crystallization rates, we may develop a potential preparation technique for producing high performance pipe materials with improved sag-resistance. However, few relevant experimental research works have been reported.

In the present study, we introduced a small amount of UHMWPE into a commercial bimodal PE-100 pipe resin by melt blending. The aim of this work is to clarify the effect of ultra high molecular weight component on the crystallization of bimodal HDPE. The isothermal and nonisothermal crystallization behaviors of physically blended HDPE/UHMWPE composites were studied with differential scanning calorimetry (DSC). The DSC thermograms provided necessary crystallization kinetics data which were further analyzed by the Avrami method. Using successive self-nucleation and annealing (SSA) thermal fractionation technique, changes in chain structures induced by UHMWPE were obtained. The spherulitic morphologies of neat HDPE and HDPE/UHMWPE composites during isothermal crystallization were observed by polarized optical microscopy (POM). Rheological measurements were also performed to evaluate the processing property of the composite.

2. Experimental

2.1. Materials and sample preparation

HDPE 4803T, a commercial bimodal PE-100 pipe resin provided by Yangzi Petrochemical Co., SINOPEC (Nanjing, China) was used in this study. Its melt flow rate (MFR) is 0.04 g/10 min (190 °C, 2.16 kg load) with a density of 0.948 g/cm³. UHMWPE powders with molecular weight $M_w = 3.5 \times 10^6$ g/mol were kindly provided by Second Auxiliary Factory of Beijing (China).

The HDPE granules and UHMWPE powders were melt-blended by a Brabender Mixer (PLE651) at a speed of 45 rpm and a mixing temperature of 165 °C for 7 min. During this period, a constant value of torque was obtained for the homogeneous blend. The HDPE samples containing 0.5 wt%, 1.0 wt%, 2.0 wt% and 3.0 wt% of UHMWPE were prepared and denoted as UHMWPE-0.5, UHMWPE-1.0, UHMWPE-2.0, UHMWPE-3.0, respectively. The neat HDPE granules were subjected to an identical mixing process for the purpose of comparison.

2.2. Calorimetric experiments

The calorimetric experiments were carried out using a Q-100 differential scanning calorimeter (DSC) (TA Instruments). Calibration for the temperature scale was performed using indium ($T_m = 156.60$ °C and $\Delta H_f^0 = 28.45$ J/g) as standard to ensure reliability of the data obtained. The temperature inaccuracy of the apparatus is ± 0.05 °C. All the experiments were carried out in nitrogen atmosphere.

2.2.1. Crystallization and melting behavior characterization

Samples were sealed in aluminum pans for DSC measurements. To minimize the thermal lag between samples and DSC furnace, each sample weighed about 10 mg. The measurements were performed following the procedure: samples were heated to 160 °C at 10 °C/min and kept at this temperature for 5 min to erase any previous thermal history. Then samples were cooled to 25 °C at 10 °C/min to determine the initial crystallization temperature (T_c^i) at the onset of the crystallization. The melting point (T_m) was taken at the melting endotherm peak of the second heating cycle after erasing the thermal history. The melting enthalpy (ΔH_m) was determined by linear interpolation of the baseline between the clear-cut end of the melting endotherm and its onset arbitrarily taken at 70 °C for all samples [31].

Isothermal crystallization study has been carried out according to the following procedure: (a) samples were heated to 160 °C and kept for 5 min to standardize the physical state of the materials prior to the experiment. (b) Fast cooling down to a desired crystallization temperature was operated at 40 °C/min. (c) Samples were isothermally kept for a period of time necessary to complete the crystallization. For each run, the heat released during crystallization was recorded as a function of time, at different given crystallization temperatures.

2.2.2. SSA thermal fractionation

The SSA procedure used for the thermal treatment of neat HDPE and HDPE/UHMWPE composites involved a series of heating–annealing–cooling cycles. (a) Samples were firstly heated to 160 °C at 10 °C/min and kept at this temperature for 5 min to erase previous thermal history. (b) Samples were cooled to 25 °C at 10 °C/min to create an initial “standard” state and kept at this minimum temperature for 5 min. (c) Samples were heated to a selected self-seeding temperature at 10 °C/min and kept at this temperature for 5 min. This step results in partial melting and annealing of unmelted crystals, while some of the melted species may isothermally crystallize [32]. (d) Crystallization after self-nucleation

was achieved by subsequently cooling the samples to 25 °C at 10 °C/min. The heating–annealing–cooling cycle was repeated at a self-seeding temperature interval of 5 °C from 140 °C to 30 °C. Finally the thermally treated samples were heated from 25 °C to 160 °C at 10 °C/min and the corresponding endothermic curves were recorded.

2.3. Polarized optical microscopy

Morphologies of neat HDPE and HDPE/UHMWPE composites were observed using an Olympus BX-51 polarized optical microscope with a Linkam-THMS600 hot stage. The sensor accuracy of the hot stage is ± 0.1 °C. Samples were melted at 200 °C and squeezed to films. These films were kept in hot stage between two microscope slides. Each sample was heated to 200 °C at 10 °C/min and kept at this temperature for 5 min to allow complete melting. Samples were subsequently cooled to a desired isothermal crystallization temperature at 40 °C/min. The nitrogen gas was purged through the hot stage during measurements.

2.4. Rheological experiments

The rheological measurements were carried out using an ARES Strain-Controlled Dynamic Torsion Rheometer, equipped with TA Orchestrator software. The torque resolution and strain resolution is 1 nN m and 0.04 μ rad, respectively. The inaccuracy of temperature control is ± 0.1 °C. Samples for rheological measurements were compression-molded to 25-mm disks at 200 °C using a laboratory mixing molder (LMM). Dynamic frequency sweeps were carried out in nitrogen at 160 °C and 190 °C with parallel plate geometry. The angular frequency (ω) varied from 0.03 rad/s to 100 rad/s. A single shear strain of 1.0% and a gap height of 1.7 mm were applied for all measurements.

3. Results and discussion

3.1. Thermal properties of HDPE/UHMWPE composites

The thermal properties of neat HDPE and HDPE/UHMWPE composites were measured by a standard heating–cooling–heating procedure at an identical rate of 10 °C/min. The melting temperature (T_m), the heat of fusion (ΔH_m), the initial crystallization temperature (T_c^i) and the crystallinity (χ_c) are shown in Table 1. For samples UHMWPE-0.5–UHMWPE-3.0, as the content of UHMWPE was pretty low, the melting temperatures and the enthalpies of fusion have not substantially changed compared with neat HDPE. However, it is clear to see that the initial crystallization temperatures of UHMWPE-0.5–UHMWPE-3.0 have been elevated by about 1–1.3 °C, which implies that the introduction of a small amount of UHMWPE could promote the crystallization capability of neat

Table 1
Thermal properties of neat HDPE and HDPE/UHMWPE composites studied in this work

| Materials | T_m^a (°C) | ΔH_m^a (J/g) | T_c^b (°C) | $\chi_{c,PE}^c$ (%) |
|------------|--------------|----------------------|--------------|---------------------|
| Neat HDPE | 129.63 | 181.6 | 116.66 | 63.21 |
| UHMWPE-0.5 | 128.96 | 179.4 | 117.74 | 62.44 |
| UHMWPE-1.0 | 129.23 | 186.1 | 117.73 | 64.78 |
| UHMWPE-2.0 | 129.48 | 180.1 | 117.91 | 62.69 |
| UHMWPE-3.0 | 129.69 | 177.8 | 117.66 | 61.89 |

^a Mean value of three measurements determined from melting endotherm of DSC heating trace after erasing the previous thermal history. Calculated standard deviation (S) is within ± 0.50 °C for T_m and $\pm 4.0\%$ for ΔH_m . S is calculated according to the following equation: $S = \sqrt{(\sum(X_n - \bar{X})^2)/(n - 1)}$.

^b Mean value of three measurements determined from crystallization exotherm of DSC cooling trace after melted. Calculated standard deviation (S) is within ± 0.35 °C.

^c Determined from measured enthalpies of fusion, ΔH_m ($\Delta H_{m,PE}^0 = 287.3$ J/g). Calculated standard deviation (S) is within $\pm 2.0\%$.

HDPE by shortening the inducing time. Industrially, the elevation of initial crystallization temperature is usually achieved by adding some nucleating agents. Therefore, in this study, the UHMWPE molecules essentially act as an effective nucleating agent for HDPE matrix and increase the crystallization rate of HDPE during the nonisothermal crystallization.

3.2. Isothermal crystallization kinetics of HDPE/UHMWPE composites

The effect of a small amount of UHMWPE on the isothermal crystallization kinetics of HDPE is very important but still a question unresolved. Therefore, the isothermal crystallization behaviors of neat HDPE and HDPE/UHMWPE composites were investigated and compared in this work. The isothermal DSC curves of neat HDPE at 121.5 °C, 122.0 °C, 122.5 °C and 123.0 °C are presented in Fig. 1. The relative degrees of crystallinity (X_t) changing with crystallization time at these temperatures are also given in the inset of Fig. 1. The X_t in this study is a relative value and could be defined as follows:

$$X_t = \int_0^t (dH/dt)dt / \int_0^\infty (dH/dt)dt \quad (1)$$

where the first integral is the heat generated at time t and the second one is the total heat when the crystallization is completed. According to the results shown in Fig. 1, it is clear that the isothermal crystallization rate of neat HDPE was strongly sensitive to the crystallization temperature. For example, when the crystallization temperature was selected as 123 °C, the whole isothermal crystallization process took 180–200 min while it only took less than 40 min to complete the crystallization at 121.5 °C. For HDPE/UHMWPE composites, similar results were obtained under the same experimental condition. These results imply that the isothermal crystallization temperature should be well-chosen to ensure feasibility of the measurements and integrality of the data obtained. For the neat HDPE and HDPE/UHMWPE composites studied here, on the one hand, if lower crystallization temperature (≤ 121 °C) is chosen, the isothermal crystallization of HDPE/UHMWPE composite will be so fast that only part of the exothermic curve could be recorded because the sample starts to crystallize before the selected crystallization temperature is reached. On the other hand, isothermal crystallization at higher temperatures (≥ 123.5 °C) will be time-consuming and unsuitable for laboratory investigation. In this study, temperatures ranging from 121.5 °C to 123.0 °C have been proved to

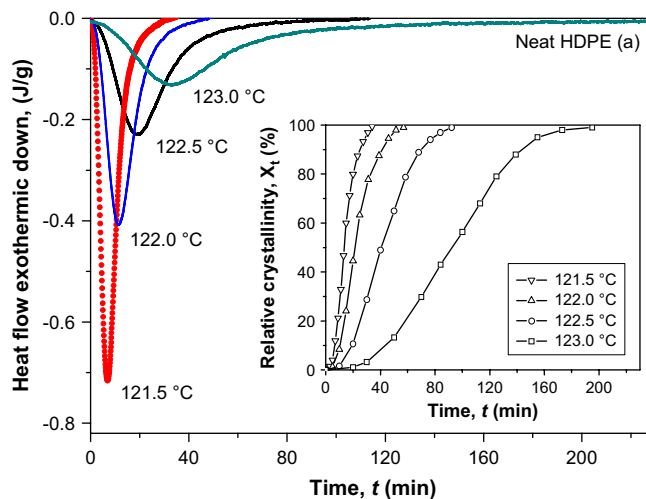


Fig. 1. The isothermal crystallization DSC curves at 121.5 °C, 122.0 °C, 122.5 °C and 123.0 °C for neat HDPE; inset shows the plot of crystallinity versus crystallization time corresponding to DSC curves.

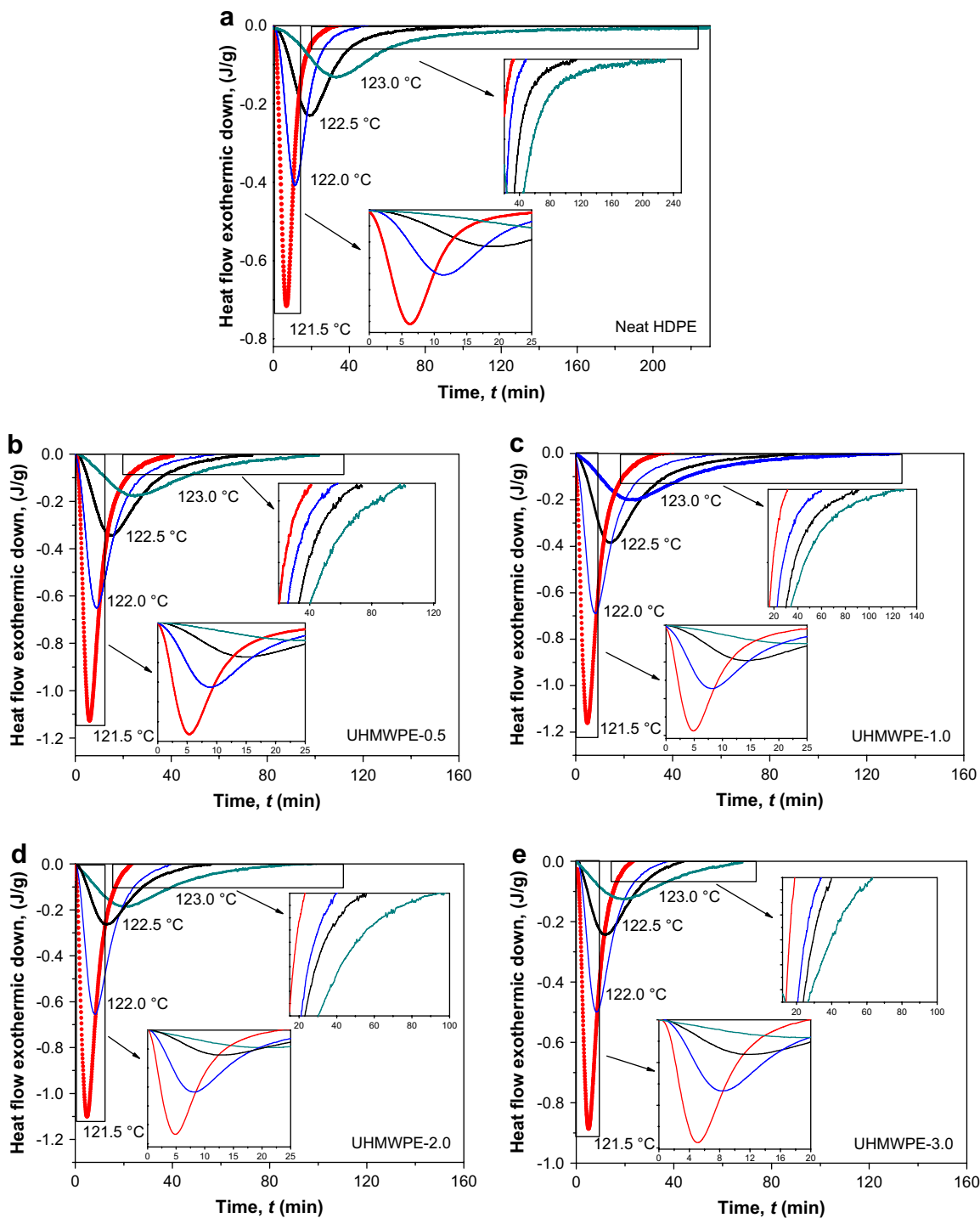


Fig. 2. Isothermal crystallization DSC curves of samples at various crystallization temperatures (a) neat HDPE, (b) UHMWPE-0.5, (c) UHMWPE-1.0, (d) UHMWPE-2.0 and (e) UHMWPE-3.0.

be appropriate for the isothermal crystallization investigations of neat HDPE and HDPE/UHMWPE composites.

The isothermal crystallization curves of neat HDPE and UHMWPE-0.5–UHMWPE-3.0 are shown in Fig. 2. It shows that the time to reach the maximum of exothermic peak of isothermal crystallization curve, t_p , decreases with the increase of supercooling temperature. Under the same crystallization temperature, the t_p values of almost all HDPE/UHMWPE composites are smaller than those of neat HDPE implying that the isothermal crystallization has been accelerated by the addition of a small amount of UHMWPE. However, it is interesting to note that at a low crystallization

temperature, such as 121.5 °C, the t_p values of neat HDPE determined from the exotherm was 6.5 min which appeared to be slightly larger than those of HDPE/UHMWPE composites which were all around 5 min. When a higher crystallization temperature was selected, for example, 123.0 °C, the t_p value of neat HDPE was close to 40 min while the values of HDPE/UHMWPE composites were all lower than 30 min. These results indicated that at lower crystallization temperature the difference of t_p between neat HDPE and HDPE/UHMWPE composites does not seem to be as prominent as that at higher crystallization temperature. It is well known that at higher crystallization temperature, the formation rate of nuclei is lower

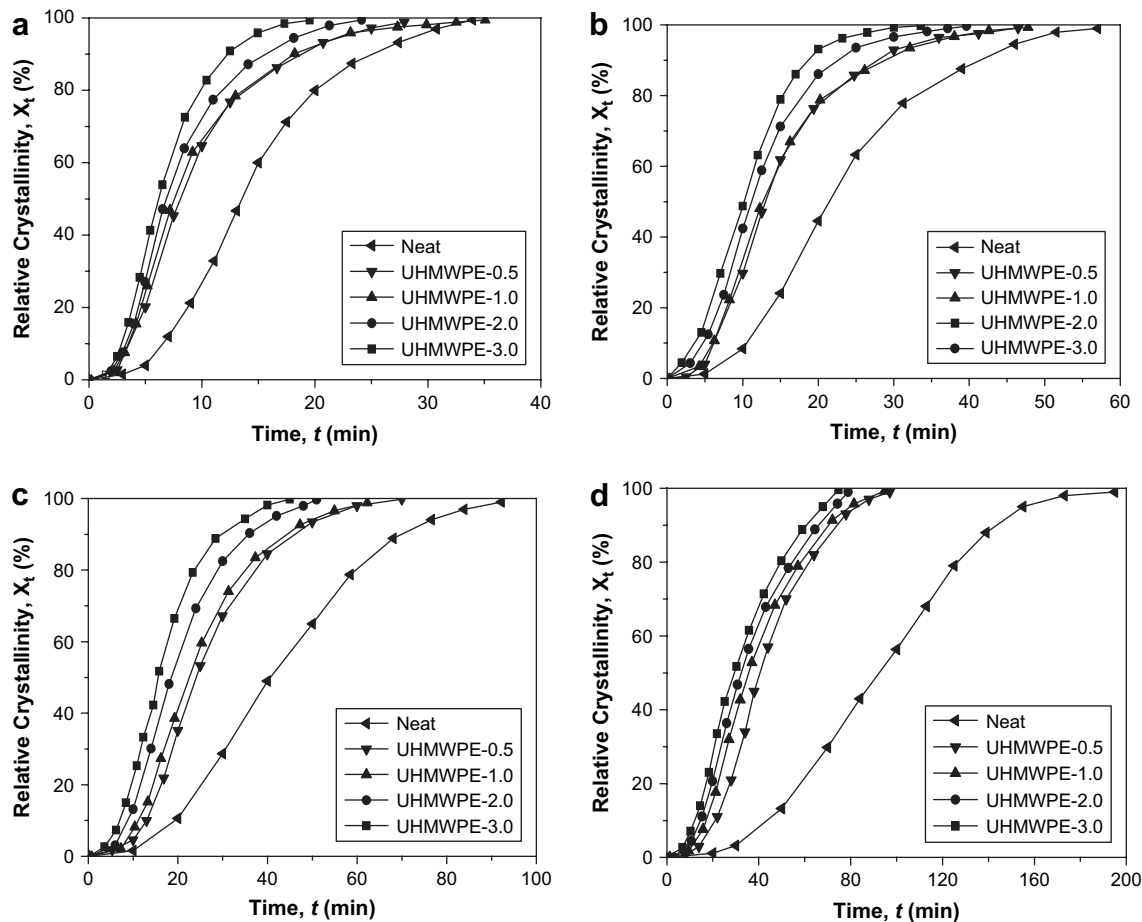


Fig. 3. The plot of X_t versus t of five samples at various isothermal crystallization temperatures (a) 121.5 °C, (b) 122.0 °C, (c) 122.5 °C and (d) 123.0 °C.

than the growth rate of crystals and the overall crystallization rate of polymer is mainly determined by the nucleation rate. Consequently, we may conclude that a small amount of UHMWPE dispersed in HDPE matrix is likely to induce the formation of more nuclei which leads to an increase of overall isothermal crystallization rate.

The plots of X_t versus crystallization time for HDPE/UHMWPE composites with different UHMWPE contents are presented in Fig. 3. It shows that within the selected isothermal crystallization temperatures, the crystallization rates of HDPE/UHMWPE composites were dependent on UHMWPE content. With UHMWPE content increased, the accelerating effect was more pronounced and the best effect was achieved for UHMWPE concentration of 3.0 wt% (sample UHMWPE-3.0) in this investigation. However, it is notable that the first addition of 0.5 wt% UHMWPE (sample UHMWPE-0.5) has a significant accelerating effect on the overall crystallization rate compared with neat HDPE: the time to reach 50% relative crystallinity, determined from $X_t - t$ plot, decreases by almost 39% at 121.5 °C and 57% at 123.0 °C. However, with further increase of UHMWPE content, the accelerating effect becomes weaker and weaker, especially at a relatively high content. For example, when the UHMWPE content increases from 2.0 wt% (sample UHMWPE-2.0) to 3.0 wt% (sample UHMWPE-3.0), the time to reach 50% X_t decreases by only 8% and 6% at 121.5 °C and 123.0 °C, respectively. These results imply that UHMWPE has an optimum content and too much UHMWPE has no more help for accelerating the crystallization process of HDPE. Therefore, in this work we choose the sample containing 3.0 wt% UHMWPE (UHMWPE-3.0) as a model composite for further analysis.

The Avrami model has been proposed to analyze the isothermal crystallization of polymers which provides a convenient approach

to explore the overall crystallization kinetics and its logarithmic form is expressed as [33],

$$\ln[-\ln(1-X_t)] = \ln K_n(T) + n \ln t \quad (2)$$

where $K_n(T)$ is the kinetic growth rate constant, n is the Avrami exponent related to the type of nucleation and to the geometry of growing crystals. Fig. 4 gives the Avrami plots corresponding to neat HDPE (a) and sample UHMWPE-3.0 (b). Theoretically, the Avrami plot should be linear and the exponent should be an integer. However, in practical situation, due to the complexity of polymer system, the Avrami plot is not always linear and the Avrami exponent is not an integer as well. From Fig. 4, we can see that each Avrami plot is composed of two linear sections. The fact indicates that there existed a secondary crystallization of HDPE and HDPE/UHMWPE composite, with the deviation which may due to the secondary crystallization that is caused by the spherulites' impingement in the later stage of crystallization process [34]. From the slope and intercept of the initial linear part, the Avrami exponent n and the rate constant $K_n(T)$ can be obtained. If the time the polymer spends from the beginning of the crystallization process to the time at which a certain amount of relative crystallinity has been developed is known, the half-time of crystallization, $t_{1/2}$, can also be directly calculated as follows:

$$t_{1/2} = \left(\frac{\ln 2}{K_n(T)} \right)^{1/n} \quad (3)$$

The values of n , $K_n(T)$ and $t_{1/2}$ of two samples at various temperatures are listed in Table 2. It can be seen that introducing 3.0 wt% of UHMWPE into neat HDPE greatly shortened $t_{1/2}$. It can also be seen

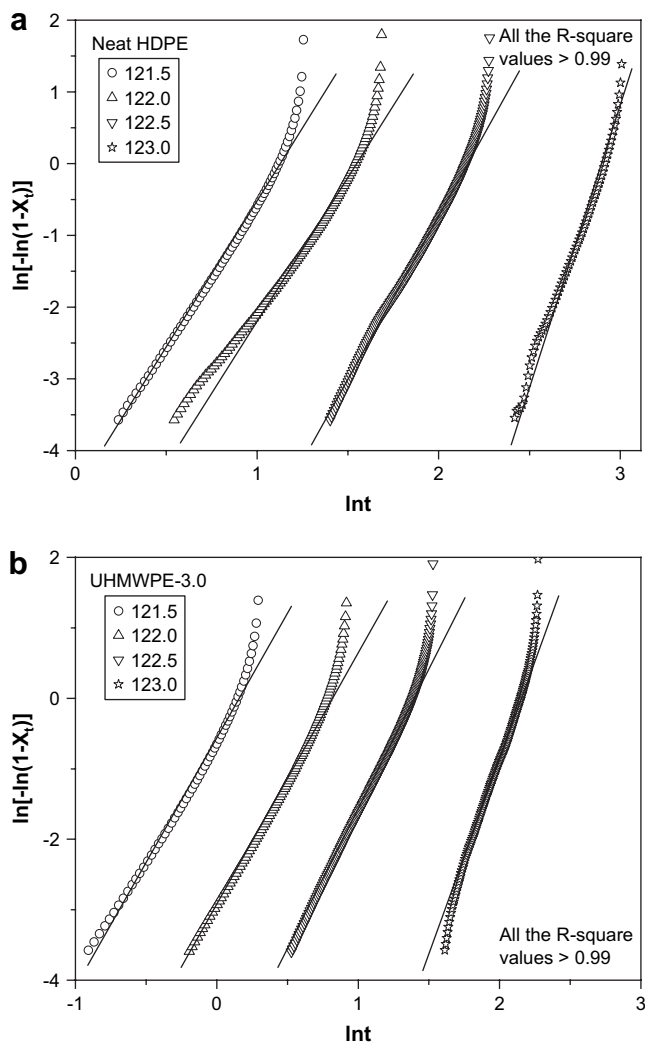


Fig. 4. Avrami plots of $\ln[-\ln(1 - X_t)]$ versus $\ln t$ for (a) neat HDPE and (b) UHMWPE-3.0, respectively.

in Table 2 that the n value of neat HDPE is around 2.8, which is slightly lower than the theoretical value 3. The depression of n could be explained by the following reasons. Firstly, for polymers with quick crystallization rate, the experimental n value will be usually lower than 3, which has been confirmed by the isothermal crystallization of neat PBT ($n = 2.6\text{--}2.9$) [35–37]. Secondly, following Vyazovkin's suggestion [38], a disadvantage of isothermal runs is that quick cooling from melting temperature to a desired temperature was followed by a period of temperature stabilization during which the crystallization kinetics remains inestimable. It should be, therefore, reasonable to treat the uncertainty in determining the initial time of crystallization processes as the main reason for a decrease in n value [39]. However, this should not influence the comparison of n values for different materials under the identical conditions. Compared with neat HDPE, the n value of HDPE/UHMWPE composites slightly increased. Krumme et al. [40] obtained similar results when they blend a low molar mass HDPE with a high molar mass HDPE. It is well known that the Avrami exponent n is in relation to type of nucleation and to the geometry of growing crystals. So these results show that the addition of UHMWPE may change the nucleation type and geometry of growing crystals of neat HDPE.

Hoffman and Lauritzen (LH) [41] had developed a dependence of the linear growth rate of spherulites, G , on the crystallization temperature T_c , that is,

Table 2

The Avrami exponent (n), crystallization half-time ($t_{1/2}$), and overall crystallization rate ($K_n(T)$), of neat HDPE and UHMWPE-3.0 at various crystallization temperatures (T_c)

| Samples | T_c (°C) | $K_n(T)$ (min ⁻ⁿ) | n^a | $t_{1/2}^b$ (min) |
|------------|------------|-------------------------------|-------|-------------------|
| Neat HDPE | 121.5 | 4.28 E-04 | 2.85 | 13.37 |
| | 122.0 | 1.47 E-04 | 2.78 | 20.96 |
| | 122.5 | 3.07 E-05 | 2.72 | 39.87 |
| | 123.0 | 2.88 E-06 | 2.76 | 89.08 |
| UHMWPE-3.0 | 121.5 | 4.40 E-03 | 2.91 | 5.69 |
| | 122.0 | 1.80 E-03 | 2.96 | 7.47 |
| | 122.5 | 1.27 E-04 | 2.96 | 18.30 |
| | 123.0 | 1.92 E-05 | 3.01 | 32.67 |

^a Mean value of three measurements. Calculated standard deviation of n is within ± 0.2 .

^b Calculated from the value of $K_n(T)$ and n .

$$G = G_0 \exp \left[\frac{-U^*}{R(T_c - T_0)} \right] \exp \left[\frac{-K_g}{T_c(\Delta T)f} \right] \quad (4)$$

where G_0 is the pre-exponential factor, U^* is the transport activation energy, $\Delta T = T_m^0 - T_c$ is the supercooling range (T_m^0 is the equilibrium melting temperature). f is the correction factor related to temperature, usually described as $f = 2T_c/(T_m^0 + T_c)$ to account for the variation in the heat of fusion per unit volume of crystals, Δh_f . T_0 is a hypothetical temperature below which all viscous flows cease, namely, $T_0 = T_g - 30$ K. K_g is the nucleation constant and can be expressed as,

$$K_g = j b_0 \sigma \sigma_e T_m^0 / k_B (\Delta h_f) \quad (5)$$

where $j = 4$ for regimes I and III growth and $j = 2$ for regime II. b_0 is the layer thickness, $\sigma \sigma_e$ is the product of lateral and fold surface free energies, Δh_f is the enthalpy of fusion, k_B is Boltzmann's constant. Using the kinetic growth rate constant $K_n(T)$ and the Avrami exponent n , Eq. (4) could be rearranged as follows:

$$\frac{1}{n} \ln K_n(T) + \frac{U^*}{R(T_c - T_\infty)} = A_n - \frac{K_g}{T_c(\Delta T)f} \quad (6)$$

Therefore we could obtain K_g by plotting the curve of $1/fT_c(\Delta T)$ versus $(1/n) \ln K_n(T) + (U^*/(R(T_c - T_\infty)))$. The obtained K_g values can be used to calculate the fold surface free energy (σ_e) of the samples from Eq. (5). The lateral surface free energy σ could be evaluated from the following empirical equation:

$$\sigma = \alpha \Delta h_f \sqrt{a_0 b_0} \quad (7)$$

where α is an empirical constant and usually assumed to be 0.1, $a_0 b_0$ represents the cross-sectional area of polymer chains, Δh_f is the volumetric heat of fusion. Δh_f , a_0 and b_0 of PE are supposed to be 2.80×10^9 erg cm⁻³, 4.55×10^{-10} m and 4.15×10^{-10} m, respectively, based on the literature [42]. It was obtained that K_g was 3.04×10^5 K² and 2.27×10^5 K² for neat HDPE and sample UHMWPE-3.0, respectively. The addition of UHMWPE gave rise to the decrease in K_g of neat HDPE. Therefore, the value of σ_e is also reduced with the decreasing K_g . The calculated σ_e value was 138.97 erg/cm² and 126.62 erg/cm² for neat HDPE and sample UHMWPE-3.0, respectively. Many researchers found that the value of σ_e could be changed by nucleating agents such as filler particles and fibers. These additives tend to promote the nucleation of spherulites on their surfaces and lead to epitaxial growth of the crystallites [43]. As a result, the value of σ_e is reduced, thereby giving rise to an increase in crystallization rate. In our experiment, the introduction of UHMWPE may act as a kind of nucleation agent which reduces the σ_e during the crystallization process and enhances the overall crystallization rate.

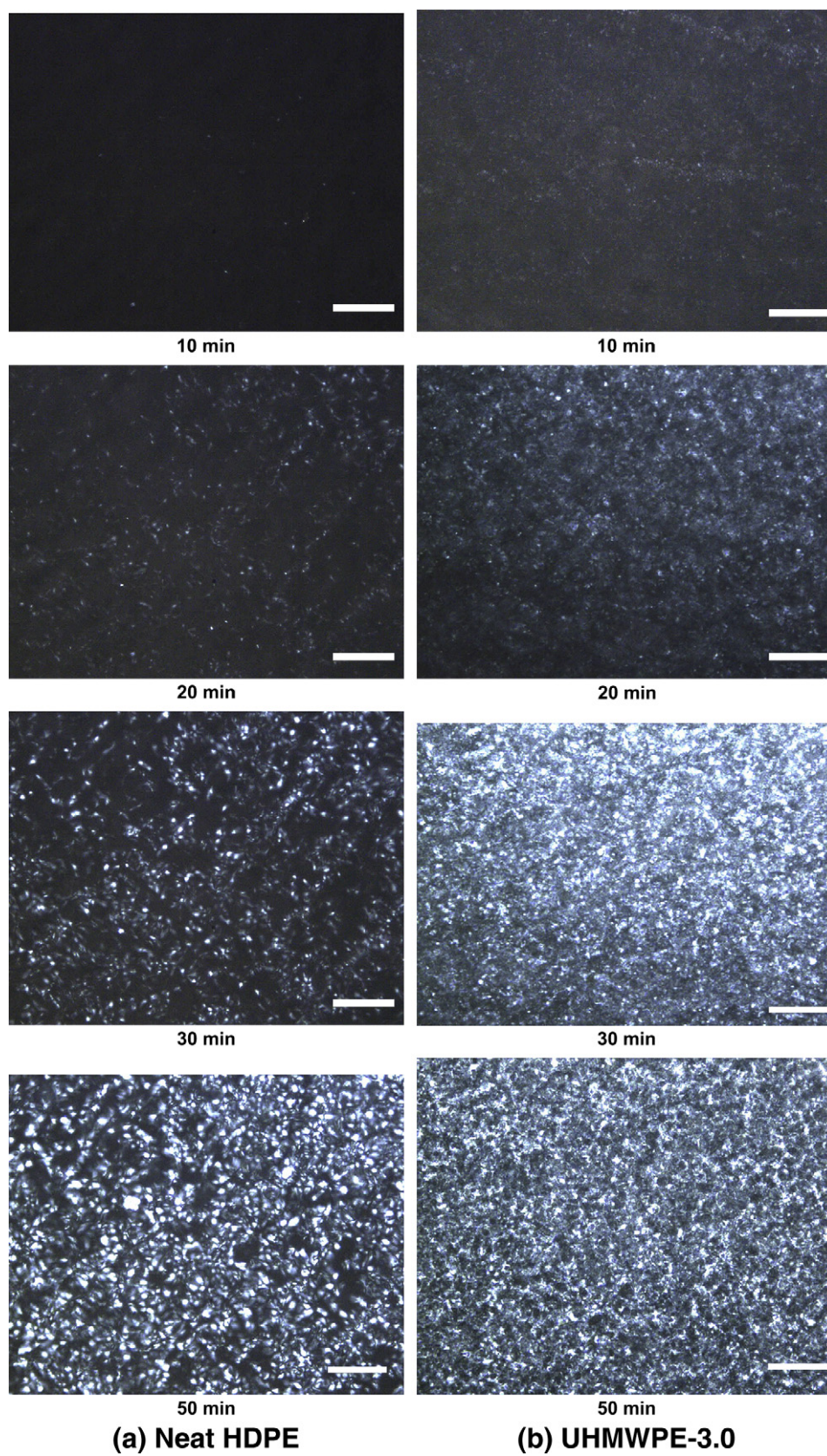


Fig. 5. Morphologies of crystallization process of HDPE/UHMWPE composite and HDPE at 129.0 °C, magnification 50 \times : (a) Neat HDPE and (b) UHMWPE-3.0. The white bar represents 50 μ m.

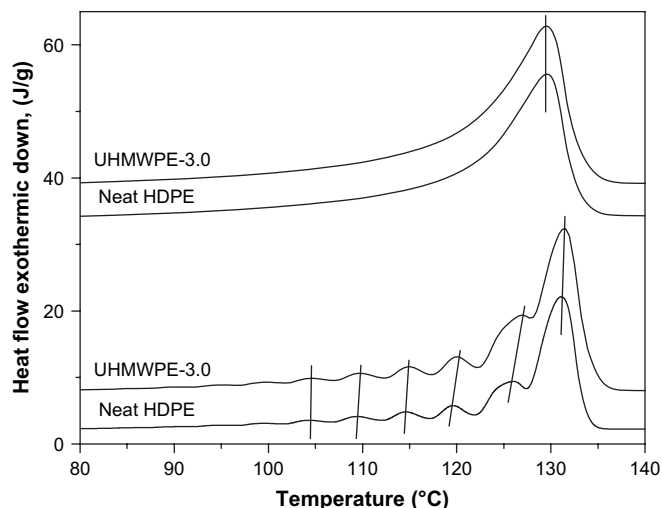


Fig. 6. DSC melting curves of neat HDPE and UHMWPE-3.0 before and after SSA thermal fractionation.

3.3. Morphologies of HDPE/UHMWPE composites

The morphological development and size of spherulites for neat HDPE and HDPE/UHMWPE composites were also investigated with polarized optical microscopy (POM). Equipped with a hot stage, real-time isothermal crystallization process could be observed and morphologies during the process could be photographed. As we have shown before, the sample UHMWPE-3.0 exhibited much faster crystallization kinetics than neat HDPE; therefore the undercooling should be well-selected to ensure a large time window for observation. The isothermal crystallization temperature was determined to be 129 °C here.

Fig. 5 displays the morphological evolution of neat HDPE and UHMWPE-3.0 during the isothermal crystallization at 129 °C. It can be seen that after 10 min of isothermal crystallization, several sporadic nuclei were visible in the neat HDPE sample. However, with regard to UHMWPE-3.0, much more nuclei appeared under the same isothermal crystallization time. At 20 min, more nuclei formed in both samples and the screen has already been full of the nuclei. Under an identical crystallization temperature, the number of nuclei formed during the same crystallization time may represent the nucleation rate of the sample. Therefore, it can be estimated that sample UHMWPE-3.0 owned a much faster nucleating rate than neat HDPE. After the formation of nuclei, the crystals tend to grow on these nuclei to form spherulites. It can be seen from Fig. 5 that at 50 min, the neat HDPE as well as UHMWPE-3.0 exhibited spherulite morphologies. However, it is also clear that the size of spherulites of UHMWPE-3.0 was much smaller than that of neat HDPE. It is known that adding nucleating agent will induce the formation of smaller crystal spherulites. POM observations were also conducted for UHMWPE-0.5, UHMWPE-1.0 and UHMWPE-2.0. Similar results were obtained. Therefore, with these results, we may conclude that UHMWPE molecules act as a kind of nucleating agent in HDPE matrix.

3.4. Thermal fractionation

Successive self-nucleation and annealing (SSA) thermal fractionation enhances the potential molecular fractionation which can occur during crystallization, while encouraging annealing of the unmelted crystals at each stage of the process, so that small effects can be magnified. This technique is based on the sequential application of self-nucleation and annealing steps to a polymer sample originally devised by Fillon et al. [32,44,45] and has been widely

used to analyze the chain structures of semi-crystallized polymers such as PE and PP [46–51]. For a SSA fractionated polymer sample, the final DSC heating run will reveal a distribution of melting points induced by thermal treatment indicating the heterogeneous nature of the chain structures of the polymer. Compared with another thermal fractionation technique so-called stepwise crystallization (SC), SSA exhibits a leading advantage that it is performed at substantially shorter times and with better resolution [52,53].

In fact, commercial bimodal HDPE resins are the mixtures of various components in which the M_w , the MWD and the short chain branched (SCB) are rather different [54]. Recently, An et al. [55] reported the influence of molecular composition on the crystallization of a sheared polyethylene. As we mentioned before, the ultra high molecular weight component may act as some kind of nucleating agent for bimodal HDPE. Therefore, the addition of UHMWPE is likely to change the chain structures of neat HDPE.

In order to understand the microstructure changes of neat HDPE after adding UHMWPE, SSA thermal fractionation was performed. The DSC heating curves of neat HDPE and sample UHMWPE-3.0 before and after SSA fractionation are shown in Fig. 6. It can be seen that, compared with untreated samples, both fractionated samples clearly exhibit a series of melting peaks that correspond to the melting of different mean lamellar thickness crystallites formed and annealed at each self-nucleation temperature employed. The Thomson–Gibbs equation [53] can be used to establish a correlation between temperature and lamellar thickness as given in the following equation:

$$l = \frac{2\sigma T_m^0}{\Delta H_v (T_m^0 - T_m)} \quad (8)$$

The equation has been used by several authors who have applied SSA fractionation [47,52,56,57]. According to Eq. (8), higher melting temperature means that thicker crystal lamellar has formed. For fractionated HDPE/UHMWPE composite, the melting temperatures of fractions between 110 °C and 140 °C are about 1–2 °C higher than those of neat HDPE. It implies that with the help of UHMWPE, the mean crystal lamellar thickness of HDPE/UHMWPE composite becomes larger. As we mentioned, SSA thermal fractionation involves a series of self-nucleation and annealing steps. UHMWPE may act as a nucleation center during these steps. Therefore, the self-nucleation and annealing process is greatly promoted by the presence of UHMWPE; more stable nuclei have been formed and growing faster with the same supercooling. As a result, thicker crystal lamellar with higher melting temperature could be obtained.

3.5. Influence of UHMWPE on rheological property

Industrially, commercially viable HDPE pipe resin must be melt processible and be able to be formed into pipe at reasonable rates and extrusion pressures. Therefore, processing property is of great importance. Usually UHMWPE does not melt and is difficult to process because melt viscosity increases rapidly with M_w . Consequently, it is necessary to consider the influence of UHMWPE on melt viscosity of HDPE/UHMWPE composites. To compare the difference in melt flow behaviors of neat HDPE and HDPE/UHMWPE composites, rheological measurements were carried out using dynamic frequency sweep mode. Fig. 7 shows the dynamic melt viscosities plots of neat HDPE and sample UHMWPE-3.0 at 160 °C and 190 °C. From the insets, we can see that the viscosity is independent of shear strain within the frequencies from 0.03 rad to 100 rad.

It is evident from Fig. 7 that neat HDPE should be easy to process since it has reasonable low viscosities at higher shear rates. Although sample UHMWPE-3.0 shows noticeably larger viscosities

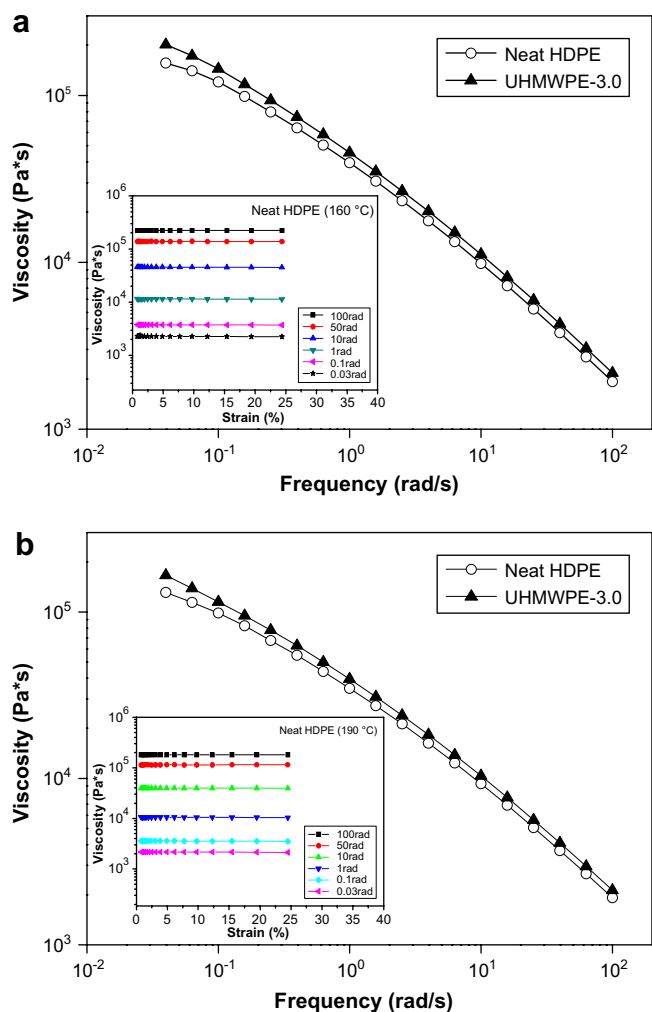


Fig. 7. The plots of dynamic melt viscosity versus frequency for neat HDPE and UHMWPE-3.0 at (a) 160 °C and (b) 190 °C. The insets show the dependence of shear strain on viscosity.

than neat HDPE at higher shear rates, it should not be difficult to process because it is shear-thinning. It could also be seen in Fig. 7 that at low shear rates close to zero, sample UHMWPE-3.0 exhibits much larger viscosities than neat HDPE sample which indicates the existence of a high molecular weight tail. The result shows that the high molecular component (UHMWPE) can effectively elevate the viscosity close to zero shear. Previous studies [4] have shown that Newtonian (zero shear) viscosity can successfully be used to model the effects of gravity-induced sag in commercial large-diameter pipe processing and an inverse relationship between zero shear viscosity and gravity-induced sag was found. Therefore, we concluded that with a small amount of UHMWPE, the zero shear viscosities of HDPE/UHMWPE composites could be elevated and the happening of gravity-induced sag during pipe manufacturing may effectively be avoided.

4. Conclusion

In this study, UHMWPE in a bimodal HDPE pipe resin acted as a kind of nucleation agent that promotes the crystallization behavior of HDPE, at a very small loading of UHMWPE, was demonstrated. The isothermal crystallization behaviors of neat HDPE and HDPE/UHMWPE composites were studied. The crystallization kinetics analyzed by the Avrami method reveals that the introduction of a small amount of UHMWPE to neat HDPE could

obviously accelerate the isothermal crystallization rate. In terms of LH theory, it is found that the fold surface free energy σ_e of HDPE/UHMWPE composite is lower than that of neat HDPE. This reduction in σ_e may attribute to the nucleating effect of ultra high molecular weight component in HDPE matrix, which conceals the possible confinement effect induced by the UHMWPE. The morphological development during crystallization clearly exhibited that the nucleation rate of HDPE is increased by the presence of UHMWPE which is in accordance with the kinetic results. The SSA thermal fractionation results showed that during self-nucleation and annealing process, the UHMWPE molecules act as some nucleating centers which help to form thicker crystal lamellar. With the results of rheological measurement, HDPE/UHMWPE composite is proved to be easy to process as neat HDPE. Moreover, at lower shear rate, the composite shows higher melt viscosity which makes it more sag-resistant.

At industrial level, the solidification times of bimodal HDPE pipe resins are crucial for both avoiding gravity-induced sag and optimizing production; hence, the nucleating effect of UHMWPE is of great importance in improving the production of bimodal HDPE pipes. Moreover, in order to well explain the nucleating action of UHMWPE in HDPE matrix at very small loading, deeper investigation should be carried out in future.

Acknowledgements

We gratefully acknowledge the financial support from the National Basic Research Program of China (G2005CB623803), the National Natural Science Foundation of China (Grant No. 50673021), the Hi-Tech Research & Development Program of China (2007AA03Z450) and the Natural Science Foundation of Shanghai (Grant No. 06ZR14007).

References

- [1] Scheirs J, Bohm LL, Boot JC, Leever PS. Trends in Polymer Science 1996;4: 408–15.
- [2] Roland S. Journal of Polymer Science, Part B: Polymer Physics 2005;43: 1729–48.
- [3] Bohm LL. Angewandte Chemie International Edition 2003;42:5010–30.
- [4] DesLauriers PJ, McDaniel MP, Rohlffing DC, Krishnaswamy RK, Secora SJ, Benham EA, et al. Polymer Engineering and Science 2005;45:1203–13.
- [5] Krishnaswamy RK. Polymer Engineering and Science 2007;47:516–21.
- [6] Xiao ZC, Akpalu YA. Polymer 2007;48:5388–97.
- [7] Tracz A, Kucinska I, Jeszka JK. Polymer 2006;47:7251–8.
- [8] Wang H. Polymer 2006;47:4897–900.
- [9] Bassett DC. Polymer 2006;47:5221–7.
- [10] Azuma M, Ma L, He CQ, Suzuki T, Bin Y, Kurosu H, et al. Polymer 2004;45: 409–21.
- [11] Bin YZ, Ma L, Adachi R, Kurosu H, Matsuo M. Polymer 2001;42:8125–35.
- [12] Valenciano GR, Job AE, Mattoso LHC. Polymer 2000;41:4757–60.
- [13] Okamoto M, Kojima A, Kotaka T. Polymer 1998;39:2149–53.
- [14] Sakurai K, Nakajo A, Takahashi T, Takahashi S, Kawazura T, Mizoguchi T. Polymer 1996;37:3953–7.
- [15] Xie SB, Zhang SM, Wang FS, Liu HJ, Yang MS. Polymer Engineering and Science 2007;45:1247–53.
- [16] Busby AJ, Zhang JX, Roberts CJ, Lester E, Howdle SM. Advanced Materials 2005; 17:364–7.
- [17] Tincer T, Coskun M. Polymer Engineering and Science 1993;33:1243–50.
- [18] Minkova L, Mihailov M. Colloid and Polymer Science 1990;268:1018–23.
- [19] Aguilar M, Martin S, Vega JF, Munoz-Escalona A, Martinez-Salazar J. Journal of Polymer Science, Part B: Polymer Physics 2005;43:2963–71.
- [20] Lim KLK, Ishak ZAM, Ishiaku US, Fuad AMY, Yusof AH, Czigan Y, et al. Journal of Applied Polymer Science 2005;97:413–25.
- [21] Lim KLK, Ishak ZAM, Ishiaku US, Fuad AMY, Yusof AH, Czigan Y, et al. Journal of Applied Polymer Science 2006;100:3931–42.
- [22] Kakiage M, Sekiya M, Yamanobe T, Komoto T, Sasaki S, Murakami S, et al. Polymer 2007;48:7385–92.
- [23] Kakiage M, Yamanobe T, Komoto T, Murakami S, Uehara H. Polymer 2006;47: 8053–60.
- [24] Zuo JD, Zhu YM, Liu SM, Jiang ZJ, Zhao JQ. Polymer Bulletin 2007;58:711–22.
- [25] Aiba M, Osawa Z. Polymer Degradation and Stability 1998;61:389–98.
- [26] Cao W, Wang K, Zhang Q, Du RN, Fu Q. Polymer 2006;47:6857–67.
- [27] Matsuba G, Sakamoto S, Ogino Y, Nishida K, Kanaya T. Macromolecules 2007; 40:7270–5.

- [28] Ogino Y, Fukushima H, Matsuba G, Takahashi N, Nishida K, Kanaya T. *Polymer* 2006;47:5669–77.
- [29] Wang JF, Wang ZG, Yang YL. *Journal of Chemical Physics* 2004;121:1105–13.
- [30] Wang JF, Zhang HD, Qiu F, Wang ZG, Yang YL. *Journal of Chemical Physics* 2003;118:8997–9006.
- [31] Hubert L, David L, Seguela R, Vigier G, Degoulet C, Germain Y. *Polymer* 2001;42:8425–34.
- [32] Muller AJ, Arnal ML. *Progress in Polymer Science* 2005;30:559–603.
- [33] Page KA, Schilling GD, Moore RB. *Polymer* 2004;45:8425–34.
- [34] Wunderlich B. *Macromolecular physics*, vol. 2. New York: Academic Press; 1997.
- [35] Gilbert M, Hybart FJ. *Polymer* 1972;13:327–32.
- [36] Pracella M, Chiellini E, Dainelli D. *Macromolecular Chemistry and Physics* 1989;190:175.
- [37] Pratt CF, Hobbs SY. *Polymer* 1976;17:12–6.
- [38] Vyazovkin S, Sbirrazzuoli N. *Journal of Physical Chemistry B* 2003;107:882–8.
- [39] Righetti MC, Munari A. *Macromolecular Chemistry and Physics* 1997;198:363–78.
- [40] Krumme A, Lehtinen A, Viikna A. *European Polymer Journal* 2004;40:359–69.
- [41] Hoffman JD, Davis GT, Lauritzen JI. In: Hannay NB, editor. *Treatise on solid state chemistry*, vol. 3. New York: Plenum; 1976. p. 497.
- [42] Hoffman JD, Miller RL. *Polymer* 1997;38:3151–212.
- [43] Tjong SC, Bao SP. *Journal of Polymer Science, Part B: Polymer Physics* 2005;43:253–63.
- [44] Lorenzo AT, Arnal ML, Sanchez JJ, Muller AJ. *Journal of Polymer Science, Part B: Polymer Physics* 2006;44:1738–50.
- [45] Fillon B, Wittmann JC, Lotz B, Thierry A. *Journal of Polymer Science, Part B: Polymer Physics* 1993;31:1383–93.
- [46] Xie YC, Zhang Q, Fan XD. *Journal of Applied Polymer Science* 2003;89:2686–91.
- [47] Kong J, Fan XD, Xie YC, Qiao WQ. *Journal of Applied Polymer Science* 2004;94:1710–8.
- [48] Zhang MQ, Wanke SE. *Polymer Engineering and Science* 2003;43:1878–88.
- [49] Starck P, Rajanen K, Lofgren B. *Thermochimica Acta* 2002;395:169–81.
- [50] Muller AJ, Arnal ML, Spinelli AL, Canizales E, Puig CC, Wang H, et al. *Macromolecular Chemistry and Physics* 2003;204:1497–513.
- [51] Zhang F, Fu Q, Lu T, Huang H, He T. *Polymer* 2002;43:1031–4.
- [52] Arnal ML, Balsamo V, Ronca G, Sanchez A, Muller AJ, Canizales E, et al. *Journal of Thermal Analysis and Calorimetry* 2000;59:451–70.
- [53] Muller AJ, Hernandez ZH, Arnal ML, Sanchez JJ. *Polymer Bulletin* 1997;39(4):465–72.
- [54] Soares JBP, Hamielec AE. *Polymer* 1995;36:1639–54.
- [55] An Y, Holt JJ, Mitchell GR, Vaughan AS. *Polymer* 2006;47:5643–56.
- [56] Zhang M, Lynch DT, Wanke SE. *Polymer* 2001;42:3067–75.
- [57] Virkkunen V, Laari P, Pitkanen P, Sundholm F. *Polymer* 2004;45:4623–31.